September 1990

Identification of Address Blocks Through Multiple Illuminations, Multiple Images and Multicolor Images

Ruzena Bajcsy
University of Pennsylvania

Helen Anderson
University of Pennsylvania

Sang Wook Lee
University of Pennsylvania

University of Pennsylvania Department of Computer and Information Science Technical Report No. MS-CIS-90-66.

Identification of Address Blocks Through Multiple Illuminations, Multiple Images and Multicolor Images

Abstract

We propose a methodology to identify the address labels on flat mail pieces, for the cases where the surface characteristics of the address label are different from the remaining surface. Two methods are used: movement of highlights with differing illumination, and identification of highlights using color information. Reasoning about changes in hue, saturation and intensity, using a new representation of color, allows us to discriminate between matte and glossy surfaces. On grayscale images, we separate diffuse reflectance areas from glossy reflectance areas, using highlights which change with illumination angle. If that does not disambiguate the label, we use color, reasoning that highlights decrease the saturation value and increase the intensity.

Comments

University of Pennsylvania Department of Computer and Information Science Technical Report No. MS-CIS-90-66.

Identification of Address Blocks Through Multiple Illuminations, Multiple Images and Multicolor Images

MS-CIS-90-66
GRASP LAB 233

Ruzena Bajcsy
Helen Anderson
Sang Wook Lee

Department of Computer and Information Science
School of Engineering and Applied Science
University of Pennsylvania
Philadelphia, PA 19104

September 1990

Identification of Address Blocks through Multiple Illuminations, Multiple Images and Multicolor Images

Ruzena Bajcsy
Helen Anderson
Sang Wook Lee

Department of Computer and Information Science
School of Engineering and Applied Science
University of Pennsylvania
Philadelphia, PA 19104

Abstract

We propose a methodology to identify the address labels on flat mail pieces, for the cases where the surface characteristics of the address label are different from the remaining surface. Two methods are used: movement of highlights with differing illumination, and identification of highlights using color information. Reasoning about changes in hue, saturation and intensity, using a new representation of color, allows us to discriminate between matte and glossy surfaces. On grayscale images, we separate diffuse reflectance areas from glossy reflectance areas, using highlights which change with illumination angle. If that does not disambiguate the label, we use color, reasoning that highlights decrease the saturation value and increase the intensity.

1 Introduction

This paper introduces a methodology to disambiguate address labels from the surrounding area, using differences in surface characteristics. The fundamental property of imaging used here is that changes in intensity and saturation can be caused by changes in illumination location and changes in surface characteristics. The first technique we use is to move the illumination or to use two cameras at different angles with the same illumination, which accomplishes the same thing (after geometric transformation). The areas of diffuse reflectance appear approximately the same, regardless of the angle between the camera and the illumination. However, areas of specular reflectance appear quite different as the angle of illumination changes. If this technique is not sufficient to differentiate address blocks, we proceed to the use of color information to identify areas of highlight. Under whitened illumination, areas of highlight have reduced saturation compared to the surrounding areas. The strength of this method is its simplicity in separation of address blocks, which lends itself to real-time applications.

In order to solve this problem, we have partitioned the problem domain into four major categories of flats, with particular interest in magazines, circulars and catalogs:

1. The label has a matte surface and the magazine is glossy.
2. The label and the magazine are both covered by plastic.
3. The matte label is on top of plastic cover.
4. The address is printed directly on the cover, and there is no label.

We believe that we have solutions for cases 1 and 3 and perhaps on some instances for case 2. If these solutions can run quickly, and we believe that they can, they will be sufficient to identify the address blocks in a substantial portion of the flats. The goal of this research is to learn to acquire images and create heuristics which have the potential to identify a large percentage of the address blocks on the flats in a running time of 0.1 to 0.3 seconds. This research does not include any address reading or special-purpose hardware for image processing, though both of those elements would be required for a complete system implementation.

The approach we use is to experiment with varying the illumination of the mail pieces, varying the camera positions, and varying the spectral information gathered from the scene. Then we will write programs which try the simplest solution, then automatically move on to the more complex heuristics which can disambiguate more and more address labels. By trying the cleanest, simplest ideas first, we plan to identify address blocks on a large fraction of the mailstream in the shortest possible time.

On glossy surfaces, highlights move when the viewing position moves, while matte surfaces (with diffuse reflectance characteristics) appear to have the same brightness from many different viewing positions. Using this knowledge, and subtracting the brightness due to diffuse reflectance from the brightness due to glossy reflectance, we have evidence that an area of matte surface can be separated from areas of glossy reflectance.

What does color information contribute to our problem? During the last two years in the GRASP laboratory we have developed a new representation of color which allows us to discriminate between matte and glossy surfaces, by reasoning about changes in hue, saturation and intensity. The color representation is described in more detail in Section 2. We have explored methods of grouping areas of similar hue, then identifying highlights based on local changes in saturation and intensity. This reasoning requires more time than subtraction techniques, and thus we use it as a secondary method rather than the first technique applied to a given piece in a mailstream.

In future work, we plan to consider edges (discontinuities) in three spaces: reflectance, hue and saturation. We will perform experiments to see whether color edges add information which is useful for address block discrimination. For example, in the absence of a glossy/matte discontinuity, sharp changes in reflectance and hue are much more likely to lead to address block discrimination than changes in saturation. We can discount the effects of saturation changes and concentrate on the effects of reflectance and hue.

Using images of mail pieces, we are in the process of testing each technique to see how far it takes us in disambiguating address labels on mail pieces. Beginning with multiple lightings, we use the difference between glossy and matte finishes to locate the address labels. However, this approach is limited by having to change the lighting of the mail piece. This could be implemented as strobe lighting, but it can be simplified by taking multiple images of one mail piece. To avoid having to multiple illuminations, we will vary the angle between the light, the object and the camera. After correcting for perspectivity, we will combine the multiple images. We will test the combination of images to see if the method is sufficient to locate address labels. After that, we will test multispectral images to see if an existing algorithm to different specular reflectance from lambertian reflectance adds more to the method. Our experiments in removal of highlights [3] on other image domains allow us to apply that to postal images. Though we have not yet implemented multiscale edge detection on color edges, this is the natural extension of the methodology. Changes in hue, saturation and value, across different spatial scales, may allow us to identify more address labels. The strength of this method is its simplicity in separation of address blocks, which lends itself to real-time application for postal applications.

2 Color

Color is one of the major features in identifying objects, and color vision has been one of the most intensively studied sensory processes in human vision. The purpose of color vision is to extract aspects of the spectral property of object surfaces in order to provide useful information in the visual process. The most notable applications in machine vision include recognition and identification of

colored objects and image segmentation, such as identification of address blocks in mail pieces.

Recently there have been approaches to the use of spectral information the detection and separation of highlights [11] [15] [25]. In the GRASP Laboratory, we have introduced an approach for the construction of a computational model for color image segmentation, not only with detection of highlights but with detection of small color changes induced by inter-reflections as well [3]. We use a metric space based on the physical properties of sensors in order to manipulate light-surface interactions.

2.1 Representation and Sensing of Color

Representation of color with finite-dimensional linear models has been a topic of many studies [6] [7] [14] [17] [22]. There have been some approaches to obtaining characteristic basis functions by investigating many samples of daylight and surface reflectances [14] [7]. It has been suggested that although the number of basis functions required to completely describe full spectra is essentially infinite, a small number of basis functions can provide good spectral approximations of most natural illuminants and surface reflectances. We use a metric space on a finite number of basis functions in order to better interpret physical properties of light-surface interactions. Both for surface reflectance and for illumination, we here employ the first three Fourier bases for their mathematical simplicity and for their sufficient effectiveness in resolving natural colors.

For the three-dimensional linear model, surface reflectance and illumination can be represented as a weighted sum of basis functions expressed as:

$$S(x,y,\lambda) = \sum_{i=0}^{2} \sigma_i(x,y) S_i(\lambda), \tag{1}$$

$$E(x,y,\lambda) = \sum_{j=0}^{2} \varepsilon_j(x,y) E_j(\lambda), \tag{2}$$

where $S_i(\lambda)$ and $E_j(\lambda)$ are the basis functions, and $\sigma_i(x,y)$ and $\varepsilon_j(x,y)$ are the scalar weighting factors at (x,y). The basis functions

$$S_0(\lambda) = 1,\ S_1(\lambda) = sin\lambda,\ S_2(\lambda) = cos\lambda \tag{3}$$

are shown in Figure 1.

The color image sensing is performed with a CCD camera using filters of different spectral responses. The measured color signal $I(x,y,\lambda)$ is obtained as a product of the spectral power distribution (SPD) of illumination $E(x,y,\lambda)$ and the surface reflectance function $S(x,y,\lambda)$, i.e.,

$$I(x,y,\lambda) = E(x,y,\lambda) S(x,y,\lambda). \tag{4}$$

With 3 filters (usually R, G and B), the quantum catch or the measured signal from the camera is given by

$$\rho_k(x,y) = \int_{\lambda_1}^{\lambda_2} I(x,y,\lambda) \cdot Q_k(\lambda) d\lambda, \tag{5}$$

where $Q_k(\lambda)$ and $\rho_k(x,y)$ for k = 0, 1, 2 are the spectral response of the $k-$th filter and the camera output through the $k-$th filter at (x,y), respectively. The wavelengths $\lambda_1 = 400\ nm$ and $\lambda_2 = 700\ nm$ cover the range of the visible spectrum. Figure 2 (a) shows the spectral response of the 3 filters: $Q_0(\lambda)$, $Q_1(\lambda)$ and $Q_2(\lambda)$. The curves are obtained from filter measurements with a spectrophotometer and are multiplied by the product of the spectral sensitivity of the CCD camera and the infra-red cut-off (IR) filter which is shown in Figure 2 (b). The filters integrate the spectral responses over the given range, and consequently act as an anti-aliasing filter in sampling the color signal [17].

With 3 basis functions, the relationship between the sensor response, illumination and reflectance is given as [18] (the spatial variables (x,y) will be omitted hereafter)

$$\underline{\rho} = \underline{\Omega^{\sigma}}\,\underline{\varepsilon} = \underline{\Omega^{\varepsilon}}\,\underline{\sigma} \tag{6}$$

where $\underline{\rho} = [\rho_0, \rho_1, \rho_2]^T$, $\underline{\varepsilon} = [\varepsilon_0, \varepsilon_1, \varepsilon_2]^T$, $\underline{\sigma} = [\sigma_0, \sigma_1, \sigma_2]^T$, and the elements of $\underline{\underline{\Omega}}^{\sigma}$ and $\underline{\underline{\Omega}}^{\varepsilon}$ in the k-th row and j-th (or i-th) column are respectively

$$\Omega^{\sigma}_{kj} = \int_{\lambda_1}^{\lambda_2} \sum_{i=0}^{2} \sigma_i S_i E_j Q_k d\lambda, \tag{7}$$

$$\Omega^{\varepsilon}_{ki} = \int_{\lambda_1}^{\lambda_2} \sum_{j=0}^{2} \varepsilon_j E_j S_i Q_k d\lambda. \tag{8}$$

To obtain the surface reflectance of objects, which is the primary information for image analysis, the influence of illumination should be discounted from the measured color in the image. This process is called color constancy. Computationally, the color constancy problem is to solve Equation (6) for $\underline{\varepsilon}$ and $\underline{\sigma}$ with the measurement $\underline{\rho}$. The solvability depends on the choice of basis functions, the number of required measurements and the number of unknowns that are determined by spatial and spectral constraints. While the general solution for color constancy with unknown illumination demands complex algorithms and some spectral and/or spatial constraints [2] [10] [16] [18] [27], it is simple to remove the known illumination color measured with a reference object. We call the process *illumination whitening*. One assumption is that the objects of interest are illuminated by light sources of the same *SPD*, and the reference object is applicable. Since we are given the product $E(\lambda)S(\lambda)$, $E(\lambda)$ and $S(\lambda)$ can be recovered only up to a multiplicative constant. This scaling ambiguity cannot be generally resolved, and thus we only solve for the spectral components of surface reflectance and illumination up to a multiplicative factor.

If we use a reference plate with known reflectance $\underline{\sigma}^{ref}$, the *SPD* of illumination obtained from

$$\underline{\varepsilon}^{ref} = (\underline{\underline{\Omega}}^{\sigma^{ref}})^{-1}\underline{\rho} \tag{9}$$

represents the spectral composition of the global illumination throughout the image area. With the normalized $\underline{\varepsilon}^{ref}_{norm} = [1,\ \varepsilon_1^{ref}/\varepsilon_0^{ref},\ \varepsilon_2^{ref}/\varepsilon_0^{ref}]^T$, the calculation of

$$\underline{\sigma} = (\underline{\underline{\Omega}}^{\varepsilon^{ref}_{norm}})^{-1}\underline{\rho} \tag{10}$$

leads to the color signal under whitened illumination expressed as:

$$I(\lambda) = \varepsilon_0 E_0(\lambda)\ [\sigma_0 S_0(\lambda) + \sigma_1 S_1(\lambda) + \sigma_2 S_2(\lambda)]. \tag{11}$$

The requirement of a reference object for illumination whitening should not be a problem for a commercial application. Calibration based on the reference object would only be needed when the illumination changed significantly. In a room with artificial light, this would not be a substantial problem.

2.2 Reflectance Model

Once the effects of color illumination have been eliminated, the color image $I(\lambda)$ represents only the surface reflectance properties multiplied by the illumination intensity ε_0.

The analysis of the color image demands proper models for various optical phenomena of surface reflections. We use the dichromatic model for dielectric materials such as plastic, paper and paint since the mail pieces are mostly dielectric [25] [12]. There are two optically different reflection mechanisms for dielectrics: surface reflection and body reflection.

- **Surface (or interface) reflection**: reflection which occurs at the interface of two materials, i.e., air and dielectrics.
- **Body reflection**: one that results from the interaction with pigments embedded inside the material.

For dielectrics, incident light is partly reflected at the surface. The surface or interface reflection occurs at the interface of air and object material. Highlights are due to the surface reflection at the surface and depend on the refractive indices of the vehicle materials. Light also partly penetrates into the material and interacts with the pigments making body reflection. The ratio of reflected and refracted light depends on refractive index of the material. The pigments determine the color of the exiting light by selectively absorbing certain wavelengths. The body and the interface reflections are spectrally different.

We can also categorize the reflections depending on the appearance as follows:

- **Specular reflection**: glossy appearance of reflection.
- **Diffuse reflection**: non-glossy pastel-like appearance.

Body reflection is always completely diffused. Therefore, it has the Lambertian property, which means that the amount of reflected light depends only on the direction of incident light with respect to the surface orientation, and that the directions of the reflected light are evenly distributed [13].

With interface reflections, on the other hand, the amount of reflected light depends both on the direction of incident light and on viewer direction with respect to the surface orientation. Interface reflections from dielectric metals have specular and diffuse components, depending on the surface finish. The degree of dispersion of light depends on the surface roughness - e.g. sandblasted surfaces are likely to have highly diffuse reflectance. However, surface roughness alone cannot make pure Lambertian properties. The reflected light still maintains a certain directionality depending on the direction of the incident light. It should be noted that the specular surface reflection is often called *specular spike* and diffuse surface reflection is called *specular lobe* [5].

In summary, body reflections occur only in dielectrics, are always completely diffused and make body color. Interface reflections can be specular or diffuse. They are spectrally flat (white) for dielectrics. The interface reflection is spectrally flat for dielectrics regardless of surface finish in the visible range of light. Body reflection, on the other hand, is spectrally colored depending on the pigments, and is always diffused. When the body reflectance is non-flat, we can detect the flat component of surface (or interface) reflectance regardless of surface roughness.

The magnitude of the image signal is also affected by geometric factors such as surface orientation $\underline{\mathbf{n}}$, illumination direction $\underline{\mathbf{l}}$ and viewing directions $\underline{\mathbf{v}}$ [13]. So far, we have assumed that the geometric factors are implicitly included either in $E(\lambda)$ or in $S(\lambda)$. More precisely, the geometrical weighting can be regarded as the local variation of illumination density on a surface patch. However, since the geometrical weighting has different mechanisms for surface and body reflections, it would be convenient to include it in the surface reflectance. If we consider the factors as part of the surface reflectance of the dichromatic model, the surface reflectance can be modeled as

$$S(\lambda) = g_S(\underline{\mathbf{n}}, \underline{\mathbf{l}}, \underline{\mathbf{v}}) S_S(\lambda) + g_B(\underline{\mathbf{n}}, \underline{\mathbf{l}}) S_B(\lambda), \tag{12}$$

where $S_S(\lambda)$ and $S_B(\lambda)$ are the surface and the body reflectance, respectively; g_S and g_B are the geometrical weighting factors for the surface and the body reflection, respectively.

Now $S_S(\lambda)$ and $S_B(\lambda)$ represent the real surface reflectance of object, i. e., *albedo*. It is well known that the observation of the surface reflection is highly dependent both on the viewer and on the illumination directions, while the body reflection depends only on the illumination direction. For most vehicle materials, the refractive index is weakly dependent on λ from 400 nm to 700 nm. Thus, $S_S(\lambda)$ is almost constant over the visible range of light, while the body color is determined by $S_B(\lambda)$.

Given that the surface reflection is flat over the spectrum, we can rewrite the color image signal as

$$I(\lambda) = (\varepsilon_0 E_0(\lambda) + \varepsilon_1 E_1(\lambda) + \varepsilon_2 E_2(\lambda))[(g_S \hat{\sigma}_{0S} + g_B \hat{\sigma}_{0B}) S_0(\lambda) + g_B \hat{\sigma}_{1S} S_1(\lambda) + g_B \hat{\sigma}_{2B} S_2(\lambda)], \tag{13}$$

where

$$\sigma_0 = g_S \hat{\sigma}_{0S} + g_B \hat{\sigma}_{0B}, \quad \sigma_1 = g_B \hat{\sigma}_{1B}, \quad \sigma_2 = g_B \hat{\sigma}_{2B}. \tag{14}$$

By using color constancy, we can remove the terms $\varepsilon_1 E_1$ and $\varepsilon_2 E_2$.

2.3 Reflection Components in the Color Space

For identification of the surface reflection mechanisms explained above, we represent the color on the orthogonal 3-dimensional space (S_0, S_1, S_2) which we call **S** space as shown in Figure 3 (a). The **S** space is an opponent space which is convenient for describing intensity, hue and saturation. The definitions of intensity, saturation and hue for our work are defined as [8]:

$$\begin{array}{lcl} \text{intensity} & = & \sigma_0, \\ \text{hue} & = & \arctan\frac{\sigma_2}{\sigma_1}, \\ \text{saturation} & = & \frac{|\sigma_{12}|}{\sigma_0}, \\ & & \text{where } |\sigma_{12}| = \sqrt{(\sigma_1^2+\sigma_2^2)}. \end{array} \tag{15}$$

Shading Shading on surfaces of uniform color is due to variations in geometry G in $g_B(\underline{\mathbf{n}},\underline{\mathbf{l}})$ in Equation (12). As can be seen in Equation (13), the shading can be modeled as the weighting of $\hat{\sigma}_{0B}$, $\hat{\sigma}_{1B}$ and $\hat{\sigma}_{2B}$ by the scaling factor g_B. Therefore a group of shaded color points in the **S** space form a linear cluster as shown in Figure 3 (b). With shading the saturation value does not change over a region.

Shadows are due to the screening of illumination by other objects, which can be modeled as the variation of ε_0, ε_1, and ε_2 (only ε_0 under whitened illumination) in Equation (13).

This shadow model is correct only when all the illumination sources have the same SPD as we assumed earlier. When there are many illumination sources of different SPD's, partial screening of lights from some sources can change spectral combination of illuminations that a shadowed surface patch receives, thus the hue and saturation values can be affected.

Highlight Since the surface reflectance is spectrally flat for dielectrics, the illuminating light is reflected from the surface without any change of color. Under white (or whitened) illumination, highlights add whiteness (σ_{0S}) to the body colors depending on $g_S(\underline{\mathbf{n}},\underline{\mathbf{l}},\underline{\mathbf{v}})$. As the result, the color points by the highlights in the **S** space are shifted upward along the S_0 direction from the linear cluster of shading as shown in Figure 3 (b). The color points of highlights and shading form planar cluster in the **S** space. The plane is perpendicular to the S_1-S_2 plane under white or whitened illumination. Since the points are shifted upward, the saturation values are always decreased by highlights compared to those of the points without highlights, while intensity is always increased.

3 Surface Analysis Using Multiple Lightings

3.1 Experimental Setup

We make a simple approach to detection of highlights by the difference in intensity and saturation between two images from two light sources. In dull matte surfaces body reflection results from the scattering of light equally in all directions, such that they appear to have the same brightness from all viewing angles. Lambert's law relates the reflected light I_B to the cosine of the angle between the light source direction $\underline{\mathbf{l}}$ and the surface normal $\underline{\mathbf{n}}$ [9] as

$$I_B = \varepsilon_0(\underline{\mathbf{n}}\cdot\underline{\mathbf{l}})S_B(\lambda). \tag{16}$$

On the other hand, in surface reflectance, the angle of incidence of light equals the angle of reflection, and there is a rapid fall-off in intensity of reflected light as the viewing angle departs from the angle of reflection. Our initial experiment consists of two light sources mounted diagonally above a mail piece on opposite sides of the piece, as shown in Figure 4. A camera is next to one light source. Two images are taken, each with one of the lights turned on. Thus both images contain similar Lambertian reflectance but widely different surface reflectance. We can subtract the effect of surface reflectance from the intensity image.

In Figure 4, the light source 1 should generate highlights in all possible shiny surfaces, Although the magazines are globally 2-dimensional, warping of the magazine cover makes small variation in

$\underline{\mathbf{n}}$. Therefore a point illumination source may fail to generate highlights in the warped area. With an assumption of orthographic projection of the camera, we have fixed angle of observer $\underline{\mathbf{v}}$, and the light directions for surface reflection are given by

$$\underline{\mathbf{l}} = 2\underline{\mathbf{n}}(\underline{\mathbf{n}} \cdot \underline{\mathbf{v}}) - \underline{\mathbf{v}} \tag{17}$$

In order to produce highlights in all the possibly warped area, we need the extended source 1 covering all the directions of $\underline{\mathbf{l}}$. The distribution of the surface orientations due to warping can be experimentally determined with many samples of magazine covers and the size and the location of the light source 1 can be designed with Equation (17). Roughened surface generates highlights at $\underline{\mathbf{v}}$ for some ranges of $\underline{\mathbf{l}}$. This can be modeled using the Torrance-Sparrow model. Therefore the light source can be narrower than the one for the glossy surfaces. Once the light source is designed for a highly glossy surfaces, it will generate highlights for roughened surfaces. Light source 2, on the other hand, should not generate any highlights on the surface. Thus it is advantageous to use a narrow size of light to avoid the possible angles for surface reflection.

With light source 1, the irradiance from the magazine cover is given by

$$I_{B_1} + I_{S_1} = S_B(\lambda) \int (\underline{\mathbf{n}} \cdot \underline{\mathbf{l}}_1) d\Omega + g_S(\underline{\mathbf{n}}, \underline{\mathbf{l}}, \underline{\mathbf{v}}) S_S(\lambda), \tag{18}$$

where I_{B_1} is the amount of body reflection and I_{S_1} is that of surface reflection. From light source 2, we have only body reflection as

$$I_{B_2} = S_B(\lambda) \int (\underline{\mathbf{n}} \cdot \underline{\mathbf{l}}_2) d\Omega \tag{19}$$

3.2 Identification of Surface Properties

Identification of surface properties is based on the observations that (under white illumination)

- Shading, highlights and shadow change the intensity,
- Shading and shadow do not change the hue or the saturation value,
- Highlight always decreases the saturation value, and increases intensity,

As explained earlier, shading and shadow do not change the saturation value of an object region with a given color. On the other hand, highlights increase only σ_0 under white illumination, thereby always decreasing the saturation. Therefore we can identify the glossy surfaces by comparing the either intensity or saturation images (or both) with two different light sources.

If light source 2 in Figure is designed to make the amount of the body reflection in Equation (18) close to the one by the source 1 in Equation (19, the difference between the two equations are mainly the large surface reflection in Equation 18. Nevertheless there can be errors due to the differences in the body reflections between the views 1 and 2. The saturation values are decreased by highlights regardless of the intensity levels. Therefore the saturation values are reliable for identifying highlights for colored materials, and the use of saturation increases the confidence of classification.

Figure 5 shows one of our initial results. Figure 5 (a) and (b) show the intensity images with light sources 1 and 2, respectively, and Figure 5 (c) shows the area of large difference due to highlights and Figure 5 (d) is the area of body reflection. Note that warping of the magazine cover reduced the surface reflection with light source 1, which indicates an improperly designed light source. Even in th3 case that a large portion of the mail piece exhibits surface reflection and a small portion does not, we can make a reasonable guess that the address label is the small matte area.

Figure 6 shows another result with better designed light source 1. Figure 6 (a) and (b) show the intensity images with the light sources 1 and 2, respectively, and Figure 6 (c) and (d) show the saturation images with the light sources 1 and 2, respectively. Figure 6 (e) shows the area of large difference in intensity and saturation due to highlights and Figure 6 (f) is the area of body reflection. Note that the better illumination source 1 generates highlights compensating for the warping of the magazine cover.

Our subsequent experiment consists of two cameras mounted diagonally above a mail piece, at the same distance from the mail piece but on opposite sides. The light source is next to one camera. We plan to register the two images by compensating for perspective distortion, then to use the same subtraction technique to identify the matte versus the glossy areas. The advantage of the multi-camera approach is that no flashing lights would be required in the real-time implementation. There would be no problem with decay time for illuminant, and so on. On the other hand, registering the two images is the difficult part of this experiment. With the assumption that the mail piece is basically flat, we think we can accomplish that task quickly and accurately.

Additional experiments will use multiple light sources and different camera locations. Some magazine surfaces are not completely flat, but instead are warped by the effects of moisture or are folded in such a way that they are taller on one side than the other. In those cases, additional light sources may allow us to separate the matte from the glossy surfaces. Also, as discussed in the section on color, we may wish to use several filters on the cameras to obtain multispectral informaion, and this will need to be corrected for perspective distortion as well.

4 Conclusion

We have shown that surface properties of matte and glossy surfaces allow discrimination of address blocks in the cases where the address block has surface properties which are different from the surrounding material. Because of the nature of image formation, changes in intensity and saturation can be caused by differences in surface characteristics over the mail piece, depending on the location of the illuminant. We exploit these changes by taking sequential grayscale images of a mail piece with different illuminants to identify differences in surface properties. The intensity of areas of specular reflectance changes substantially when the illumination source is moved, but the intensity of matte surfaces stays approximately the same. To speed this technique, we presented the concept of using simultaneous images of mail piece taken from different locations, which gives the multiple lighing effect but requires a geometric transformation of the image data for proper registration. If the multiple lighting technique is insufficient, we proceed to color images. Areas of specular reflection have reduced saturation in comparison with matte areas. These techniques are appropriate for initial estimates of address block location.

5 Acknowledgement

This work was in part supported by DARPA Grant N0014-88-K-0630 (administered through ONR), AFOSR Grants 88-0244, AFOSR 88-0296; Army/DAAL 03-89-C-0031PRI; NSF Grants CISE/CDA 88-22719, IRI 89-06770, IRI89-17721; and Du Pont Company.

6 Bibliography

References

[1] H.L. Anderson, "GRASP Lab Camera Systems and their Effects on Algorithms," *GRASP Laboratory Technical Report MS-CIS-88-85*, University of Pennsylvania, October, 1988.

[2] R. Bajcsy, S.W. Lee, A. Leonardis, "Computational Aspects of Color Constancy," *GRASP Laboratory Technical Report MS-CIS-89-50*, University of Pennsylvania, September, 1989.

[3] R. Bajcsy, S.W. Lee, A. Leonardis, "Color Image Segmentation with Detection of Highlights and Local Illumination Induced by Inter-reflections," *Proc. of the 10th International Conference on Pattern Recognition*, Atlantic City, NJ, June 16-21, 1990.

[4] R. Bajcsy, K. Wohn, F. Solina, A. Gupta, P. Sinha, C.J. Tsikos, "Second Interim Technical Report for Advanced Research in Range Image Interpretation for Automated Mail Handling," *GRASP Laboratory Technical Report MS-CIS-88-43*, University of Pennsylvania, 1988.

[5] P. Beckman and A. Spizzichino, **The scattering of Electromagnetic Waves from Rough Surfaces**, Pergamon Press, Oxford, England, 1963. Florida, 1988.

[6] G. Buchsbaum and A. Gottschalk, "Chromaticity Coordinates of of Frequency-limited Functions," *Journal of the Optical Society of America* **1**, pp 885-887, 1984.

[7] J. Cohen, "Dependency of the Spectral Reflectance Curves of the Munsell Color Chips," *Psychon. Sci.* **1**, pp 369-370, 1964.

[8] M. D'Zmura and P. Lennie, "Mechanisms of Color Constancy," *Journal of the Optical Society of America* **3**, No. 10, pp 1662-1672, October, 1986.

[9] J.D. Foley, A. Van Dam, **Fundamentals of Interactive Computer Graphics**, Addison-Wesley Publishing Company, 1982.

[10] D. A. Forsyth, "A Novel Approach to Colour Constancy," *Proceedings ICCV* **2**, pp 9-18, Tampa, 1988.

[11] R. Gershon, *The Use of Color in Computational Vision*, PhD dissertation, Department of Computer Science, University of Toronto, 1987.

[12] G. H. Healey and T. O. Binford, "Predicting Material Classes," *Proceedings of the DARPA Image Understanding Workshop*, Pittsburgh, pp. 1140-1146, 1988.

[13] B.K.P. Horn, **Robot Vision**, The MIT Press, 1986.

[14] D. B. Judd, D. L. MacAdam, and G. W. Wyszecki, "Spectral Distribution of Typical Daylight as a Function of Correlated Color Temperature," *Journal of the Optical Society of America* **54**, pp 1031-1040, 1964.

[15] G. J. Klinker, S. A. Shafer and T. Kanade, "Image Segmentation and Reflection Analysis Through Color," *Proceedings of the DARPA Image Understanding Workshop*, Pittsburgh, pp. 838-853, 1988.

[16] L. T. Maloney, "Computational Approaches to Color Constancy," *Applied Psychology Laboratory, Technical Report 1985-01*, Stanford University, January, 1985.

[17] L. T. Maloney, "Evaluation of Linear Models of Surface Reflectance with Small Number of Parameters," *Journal of the Optical Society of America* **3**, No. 10, pp 1673-1683, 1986.

[18] L. T. Maloney and B. A. Wandell, "A Computational Model of Color Constancy," *Journal of the Optical Society of America* **1**, No. 1, pp 29-33, 1986.

[19] S.K. Nayar, K. Ikeuchi, T. Kanade, "Extracting Shape and Reflectance of Lambertian, Specular and Hybrid Surfaces," Carnegie-Mellon University Technical Report CMU-RI-TR-88-14, 1988.

[20] R. Nevatia, "A Color Edge Detector and Its Use in Scene Segmentation," *IEEE Trans. on Systems, Man, and Cybernetics* **7**, No. 11, pp 820-826, 1977.

[21] R. Ohlander, K. Price and D. R. Reddy, "Picture Segmentation Using a Recursive Region Splitting Method," *Computer Graphics and Image Processing* **8**, No. 3, pp 313-333, 1978.

[22] J. P. S. Parkkinen, J. Hallikainen, T. Jaaskelainen, "Characteristic Spectra of Munsell Colors," *Journal of the Optical Society of America* **6**, pp 318-322, 1989.

[23] J. M. Rubin and W. A. Richards, "Color Vision and Image Intensities: When are Changes Materials?" *Biol. Cybern.* **45**, pp. 215-226, 1982.

[24] J. M. Rubin and W. A. Richards, "Color Vision: Representing Material Categories," M.I.T. Artif. Intell. Lab., Massachusetts Inst. Technol., Cambridge, MA, *A. I. Memo.* **764**, 1984.

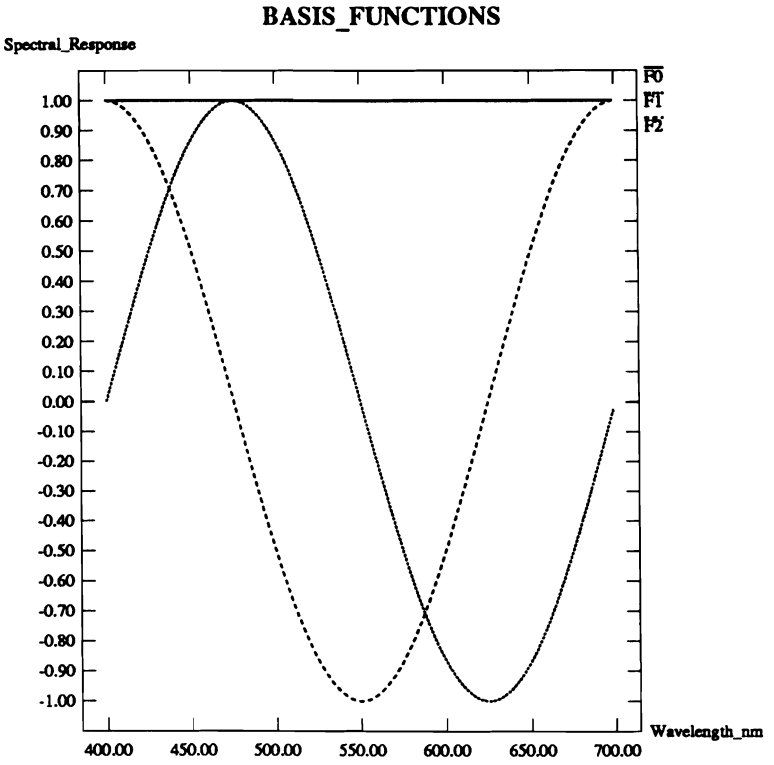

Figure 1: First three Fourier basis functions

[25] S. A. Shafer, "Using Color to Separate Reflection Components," *COLOR Research and Application*, **10**, No. 4, pp 210-218, 1985.

[26] B. A. Wandell, "The Synthesis and Analysis of Color Images," *IEEE Trans. on PAMI* **9**, No.1, pp. 2-13, 1987.

[27] A. Yuille, "A Method for Computing Spectral Reflectance," *Biological Cybernetics* **56**, pp 195-201, 1987.

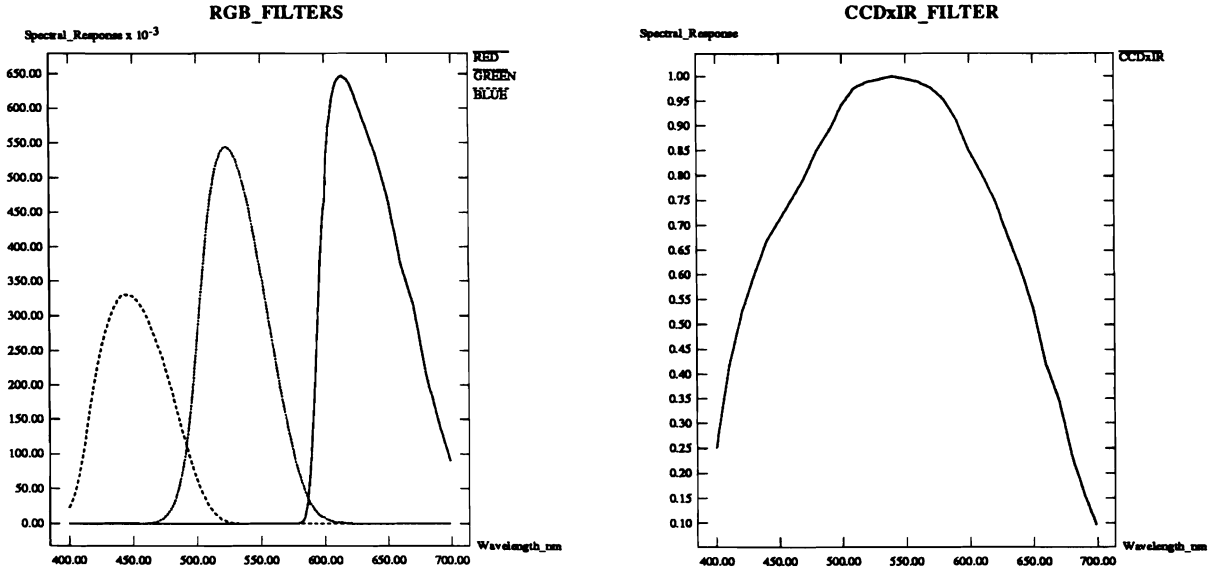

Figure 2: Measured spectral response of red, green and blue optical filters

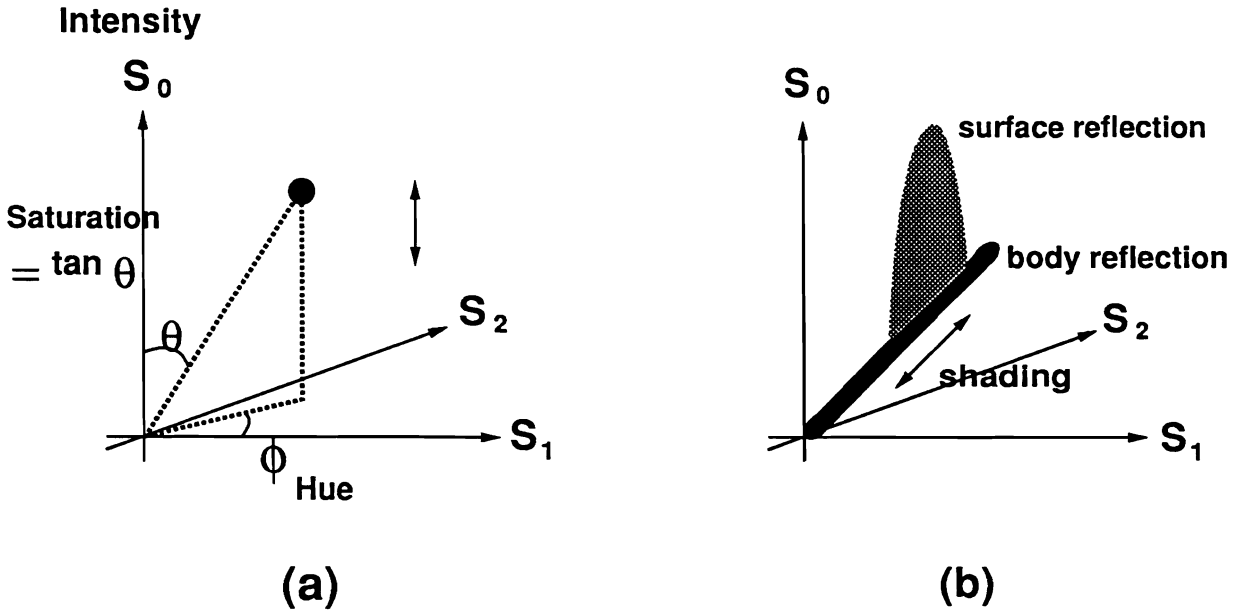

Figure 3: a Relationship between S_0, S_1, S_2 and Intensity, Saturation and Hue. b S_0, S_1, S_2 values for an object with both surface and body reflections.

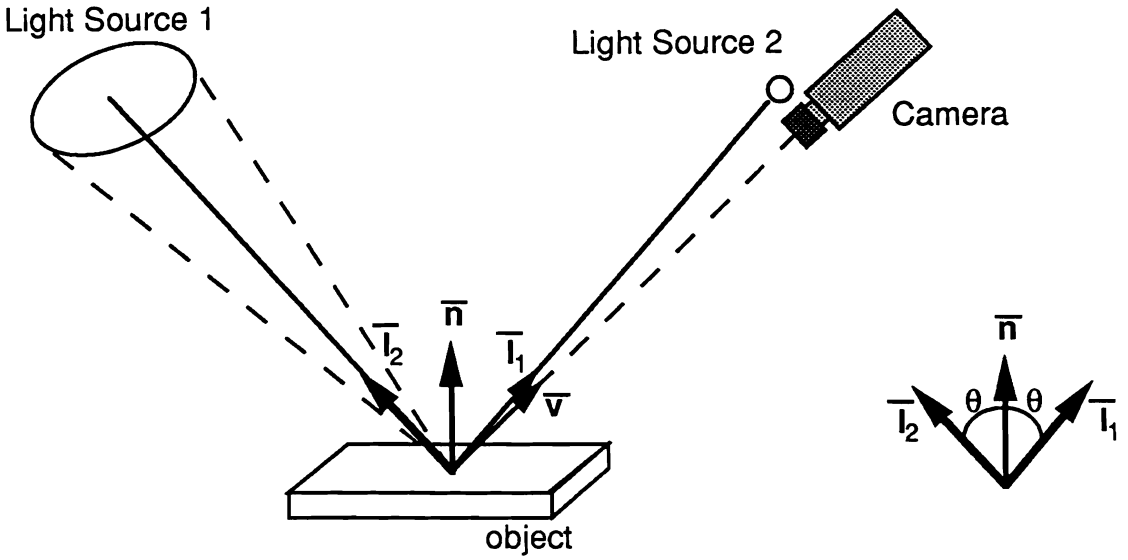

Figure 4: Experimental Setup

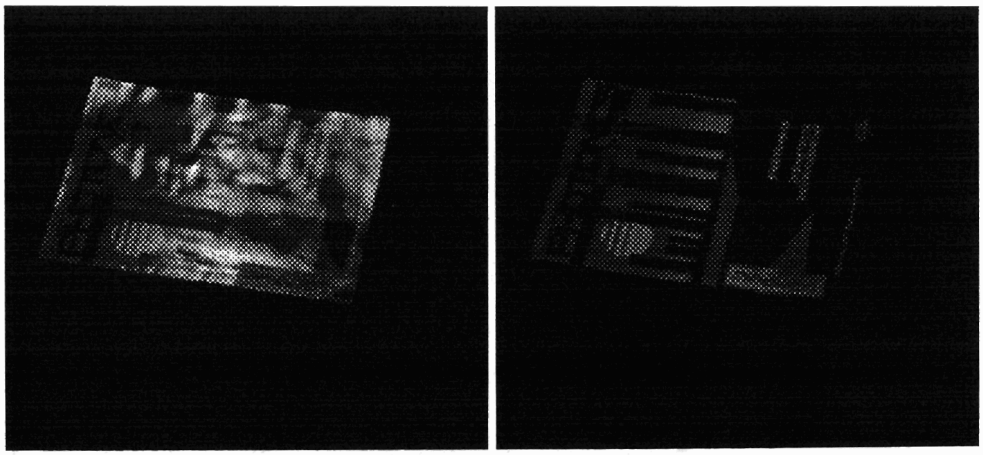

Original images with two lightings.

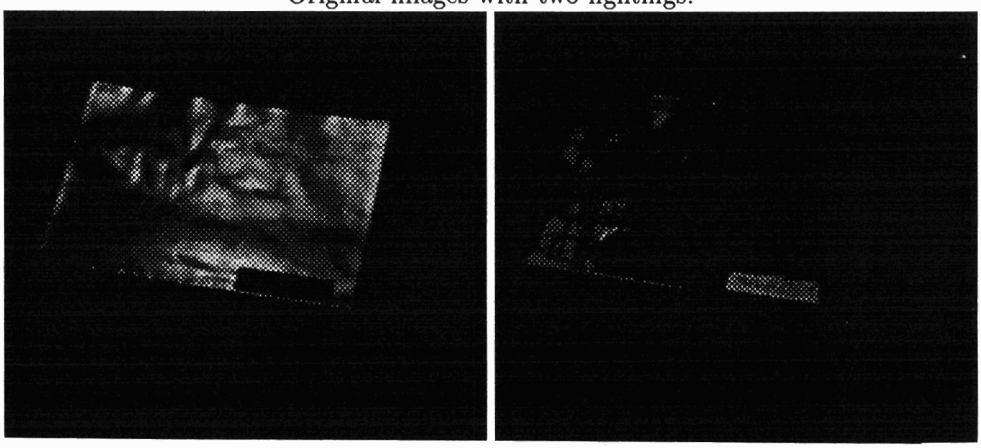

Difference, Complement of difference

Figure 5: Multiple Lighting for Address Block Location

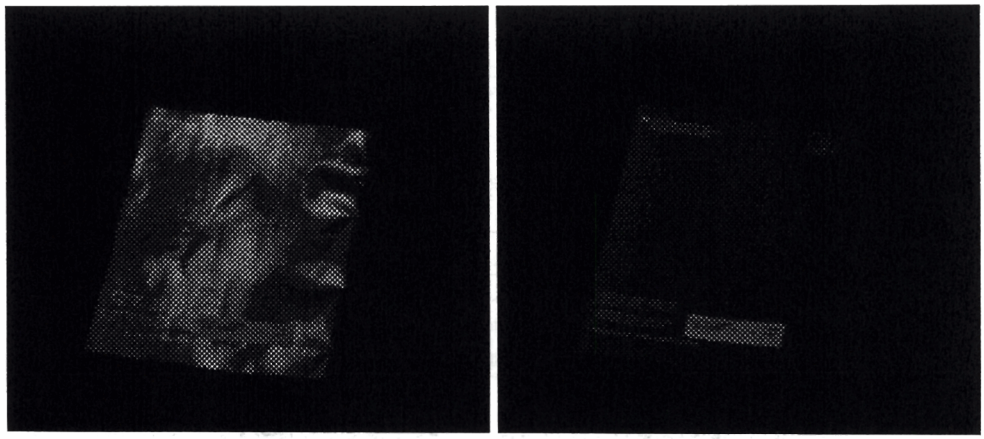

Intensity images with two lightings.

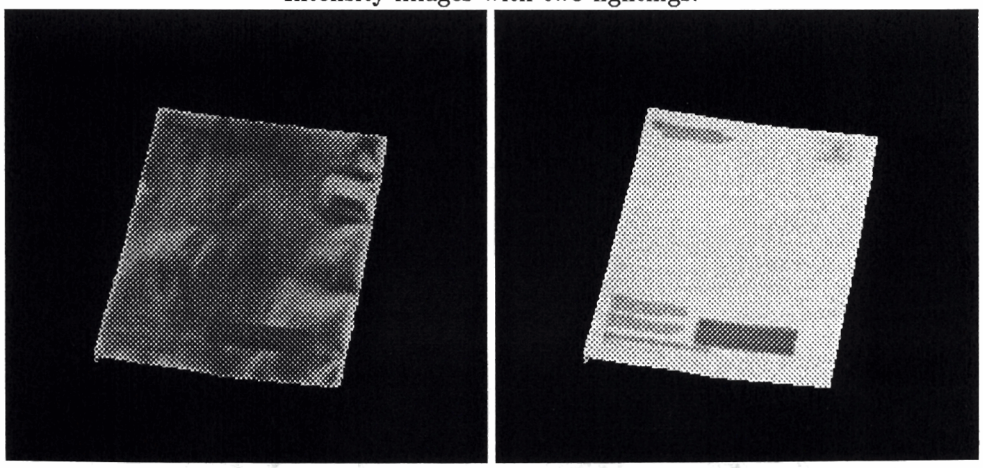

Saturation images with two lightings.

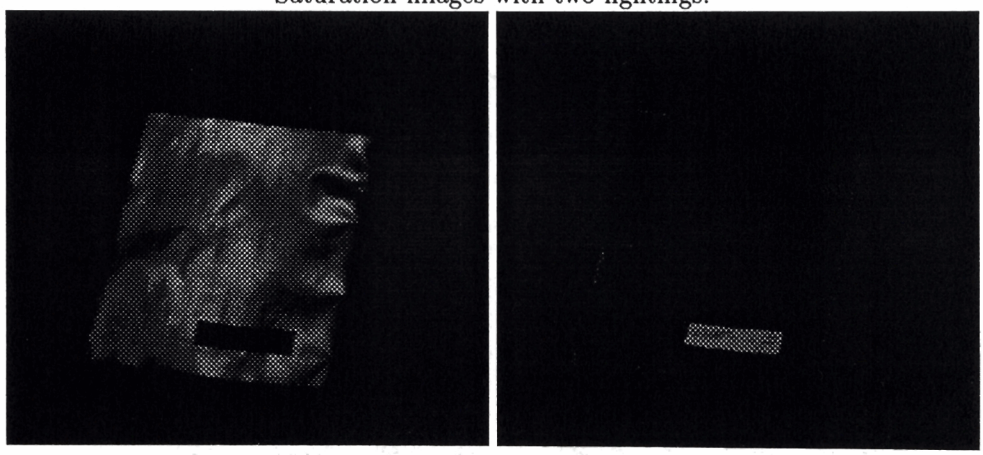

Difference, Complement of difference

Figure 6: Multiple Lighting for Address Block Location